

Krylov Linear Solvers and Quasi Monte Carlo Methods for Transport Simulations

Sam Pasmann,^a C. T. Kelley,^b and Ryan McClarren^{*,a}

*^aDepartment of Aerospace and Mechanical Engineering
University of Notre Dame
Fitzpatrick Hall, Notre Dame, IN 46556*

*^bNorth Carolina State University, Department of Mathematics
3234 SAS Hall, Box 8205
Raleigh NC 27695-8205*

*Email: rmcclarr@nd.edu

Number of pages: 12

Number of tables: 4

Number of figures: 3

Abstract

QMC + Krylov

Keywords — Quasi Monte Carlo Methods, Krylov Linear Solvers

I. INTRODUCTION

II. COMPUTATIONAL RESULTS

In this section we consider an example from [1]. The formulation of the transport problem is taken from [2]. The equation for the angular flux ψ is

$$\mu \frac{\partial \psi}{\partial x}(x, \mu) + \Sigma_t(x) \psi(x, \mu) = \frac{1}{2} \left[\Sigma_s(x) \int_{-1}^1 \psi(x, \mu') d\mu' + q(x) \right] \text{ for } 0 \leq x \leq \tau \quad (1)$$

The boundary conditions are

$$\psi(0, \mu) = \psi_l(\mu), \mu > 0; \psi(\tau, \mu) = \psi_r(\mu), \mu < 0.$$

II.A. Multigroup Equations

In general geometry the multigroup equations are

$$\mu \frac{\partial \psi_g}{\partial x}(x, \mu) + \Sigma_{t,g}(x) \psi_g(x, \mu) = \frac{1}{2} \sum_{g'=1}^G \Sigma_{s,g' \rightarrow g}(x) \int_{-1}^1 \psi_{g'}(x, \mu') d\mu' + \frac{q_g(x)}{2} \quad g = 1, \dots, G. \quad (2)$$

The boundary conditions are

$$\psi_g(0, \mu) = \psi_{l,g}(\mu), \mu > 0; \psi_g(\tau, \mu) = \psi_{r,g}(\mu), \mu < 0.$$

In matrix form, these equations are

$$\mu \frac{\partial \vec{\psi}}{\partial x}(x, \mu) + \underline{\Sigma}_t(x) \vec{\psi}(x, \mu) = \frac{1}{2} \underline{\Sigma}_s(x) \int_{-1}^1 \vec{\psi}(x, \mu') d\mu' + \frac{\vec{q}(x)}{2}, \quad (3)$$

where

$$\vec{\psi} = (\psi_1, \psi_2, \dots, \psi_G)^T, \quad \vec{q} = (q_1, q_2, \dots, q_G)^T, \quad (4)$$

$$\underline{\Sigma}_t(x) = \begin{pmatrix} \Sigma_{t,1}(x) & 0 & \dots \\ 0 & \Sigma_{t,2}(x) & 0 \dots \\ \vdots & & \ddots \\ 0 & \dots & 0 & \Sigma_{t,G}(x) \end{pmatrix}, \quad (5)$$

and

$$\underline{\Sigma}_s(x) = \begin{pmatrix} \Sigma_{s,1 \rightarrow 1}(x) & \Sigma_{s,2 \rightarrow 1}(x) & \dots & \Sigma_{s,G \rightarrow 1}(x) \\ \Sigma_{s,2 \rightarrow 1}(x) & \Sigma_{s,2 \rightarrow 1}(x) & \dots & \Sigma_{s,G \rightarrow 2}(x) \\ \vdots & \vdots & & \vdots \\ \Sigma_{s,G \rightarrow 1}(x) & \Sigma_{s,G \rightarrow 1}(x) & \dots & \Sigma_{s,G \rightarrow G}(x) \end{pmatrix}, \quad (6)$$

II.B. Source Iteration and Linear Solvers

Source iteration is Picard iteration for the fixed point problem

$$\phi = \mathcal{S}(\phi, q, \psi_l, \psi_r)$$

To use other solvers we must convert to a linear system via

$$\mathcal{K}(\phi) = \mathcal{S}(\phi, 0, 0, 0) \text{ and } f = \mathcal{S}(0, q, \psi_l, \psi_r)$$

to get

$$A\phi \equiv (I - \mathcal{K})\phi = f,$$

which we can send to a linear solver.

In the computations we use the problem from [1]

$$\tau = 5, \Sigma_s(x) = \omega_0 e^{-x/s}, \Sigma_t(x) = 1, q(x) = 0, \psi_l(\mu) = 1, \psi_r(\mu) = 0,$$

and consider two cases $s = 1$ and $s = \infty$

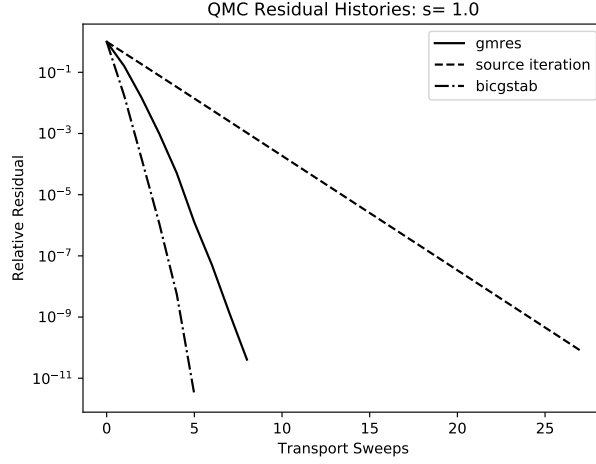


Fig. 1. $s = 1$

II.C. QMC and Krylov Linear Solvers

The linear and nonlinear solvers come from the Julia package [SIAMFANLEQ.jl](#) [3]. The documentation for these codes is in the [Juila notebooks](#) [4] and the book [5] that accompany the package.

We solve the QMC linear problem with $N=2048$ and $N_x=100$. We use two krylov methods [6], GMRES [7] and Bi-CGSTAB [8]. Figures 2 and 3 show that the Krylov iterations take fewer than half of the number of transport sweeps that Picard iteration required.

FIGURES/seqinf.pdf

Fig. 2. $s = 1$

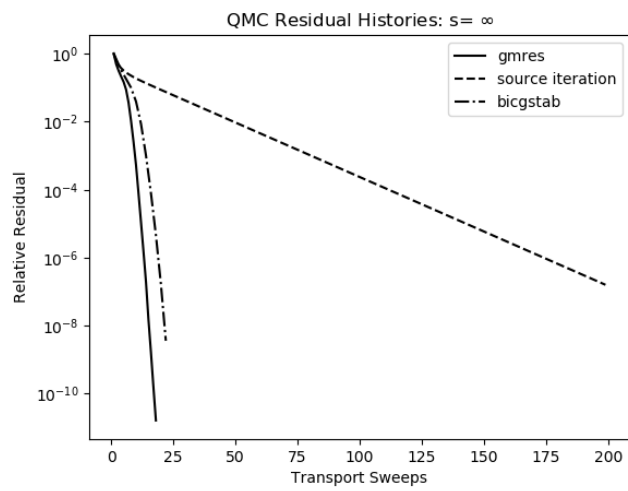


Fig. 3. $s = \infty$

II.D. Validation and calibration study

We conclude this section with a validation study. We compare the QMC results with the results from [1]. The results in [1] are exit distributions and are accurate to six figures. We have duplicated those results with an Sn computation on a fine angular and spatial mesh.

Sam, Ryan, should we use more or different values of N and Nx ?

For $N = 1000$ and $Nx = 100$ we obtain the cell-average fluxes from the QMC approximation. We then use a single Sn transport sweep to recover the exit distributions from the QMC cell-average fluxes. We report the results and the corresponding results from [1] in Tables I and II.

The exit distributions, as is clear from Table I can vary by five orders of magnitude. Even so, the results from QMC agree with the benchmarks to roughly two figures.

TABLE I
Exit Distributions: $s = 1$

μ	Garcia/Siewert		QMC	
	$\psi(0, -\mu)$	$\psi(\tau, \mu)$	$\psi(0, -\mu)$	$\psi(\tau, \mu)$
5.00e-02	5.89664e-01	6.07488e-06	5.71197e-01	5.85487e-06
1.00e-01	5.31120e-01	6.92516e-06	5.22137e-01	6.66741e-06
2.00e-01	4.43280e-01	9.64232e-06	4.41567e-01	9.25261e-06
3.00e-01	3.80306e-01	1.62339e-05	3.81029e-01	1.54416e-05
4.00e-01	3.32964e-01	4.38580e-05	3.34673e-01	4.09691e-05
5.00e-01	2.96090e-01	1.69372e-04	2.98224e-01	1.57373e-04
6.00e-01	2.66563e-01	5.73465e-04	2.68871e-01	5.35989e-04
7.00e-01	2.42390e-01	1.51282e-03	2.44749e-01	1.42448e-03
8.00e-01	2.22235e-01	3.24369e-03	2.24583e-01	3.07431e-03
9.00e-01	2.05174e-01	5.96036e-03	2.07478e-01	5.67991e-03
1.00e+00	1.90546e-01	9.77123e-03	1.92789e-01	9.35351e-03

In Tables III and IV we look at the relative errors in the QMC exit distributions as compared to a highly accurate SN result. We compensate for the widely varying scales by tabulating, for each value of N and Nx

$$R = \max(R^0, R^\tau)$$

where

$$R^0 = \max_{\mu} \frac{|\psi^{SN}(0, -\mu) - \psi^{QMC}(0, -\mu)|}{\psi^{SN}(0, -\mu)}$$

and

$$R^\tau = \max_{\mu} \frac{|\psi^{SN}(\tau, \mu) - \psi^{QMC}(\tau, \mu)|}{\psi^{SN}(\tau, \mu)}.$$

TABLE II
Exit Distributions: $s = \infty$

μ	Garcia/Siewert		QMC	
	$\psi(0, -\mu)$	$\psi(\tau, \mu)$	$\psi(0, -\mu)$	$\psi(\tau, \mu)$
5.00e-02	8.97798e-01	1.02202e-01	8.47454e-01	1.00663e-01
1.00e-01	8.87836e-01	1.12164e-01	8.52822e-01	1.10325e-01
2.00e-01	8.69581e-01	1.30419e-01	8.47710e-01	1.29064e-01
3.00e-01	8.52299e-01	1.47701e-01	8.35879e-01	1.46849e-01
4.00e-01	8.35503e-01	1.64497e-01	8.22291e-01	1.64034e-01
5.00e-01	8.18996e-01	1.81004e-01	8.08044e-01	1.80827e-01
6.00e-01	8.02676e-01	1.97324e-01	7.93459e-01	1.97336e-01
7.00e-01	7.86493e-01	2.13507e-01	7.78672e-01	2.13625e-01
8.00e-01	7.70429e-01	2.29571e-01	7.63768e-01	2.29725e-01
9.00e-01	7.54496e-01	2.45504e-01	7.48818e-01	2.45642e-01
1.00e+00	7.38721e-01	2.61279e-01	7.33889e-01	2.61361e-01

Ryan, for large N_x I see convergence as N increases. Is it clearly $1/N$? Am I missing something? Am I tabulating the wrong thing?

TABLE III
Exit Distributions Errors: $s = 1.0$

$N_x \setminus N$	1000	2000	4000	8000	16000
50	1.41162e-01	1.36428e-01	1.34747e-01	1.35736e-01	1.35577e-01
100	7.08438e-02	6.60744e-02	6.52017e-02	6.51605e-02	6.49914e-02
200	4.17171e-02	3.30480e-02	3.23088e-02	3.21432e-02	3.17467e-02
400	4.55590e-02	1.73115e-02	1.63072e-02	1.61542e-02	1.58469e-02
800	4.83754e-02	1.93087e-02	1.29178e-02	8.30117e-03	7.96562e-03
1600	5.07584e-02	2.03691e-02	1.44681e-02	4.52388e-03	4.11350e-03
3200	5.09694e-02	2.13418e-02	1.48086e-02	2.88667e-03	2.18194e-03

TABLE IV
Exit Distributions Errors: $s = \infty$

$N_x \setminus N$	1000	2000	4000	8000	16000
50	5.95648e-02	2.42755e-02	1.36521e-02	1.29509e-02	1.22769e-02
100	5.60749e-02	2.31030e-02	1.31680e-02	6.45949e-03	6.59550e-03
200	5.62864e-02	2.32524e-02	1.42149e-02	4.77319e-03	3.55246e-03
400	5.30954e-02	2.17854e-02	1.48225e-02	4.73260e-03	2.05558e-03
800	7.66264e-02	1.88155e-02	1.60082e-02	4.34610e-03	1.41402e-03
1600	5.99376e-02	2.15675e-02	1.56784e-02	4.21636e-03	1.29138e-03
3200	5.74319e-02	1.89482e-02	2.00195e-02	3.26688e-03	1.49649e-03

III. CONCLUSION

ACKNOWLEDGMENTS

The research of CTK was supported by Department of Energy grant DE-NA003967, and National Science Foundation Grants DMS-1745654, and DMS-1906446.

REFERENCES

- [1] R. GARCIA and C. SIEWERT, “Radiative transfer in finite inhomogeneous plane-parallel atmospheres,” *J. Quant. Spectrosc. Radiat. Transfer*, **27**, 141 (1982).
- [2] J. WILLERT, C. T. KELLEY, D. A. KNOLL, and H. K. PARK, “Hybrid Deterministic/Monte Carlo Neutronics,” *SIAM J. Sci. Comp.*, **35**, S62 (2013).
- [3] C. T. KELLEY, “SIAMFANLEquations.jl,” <https://github.com/ctkelley/SIAMFANLEquations.jl> (2020); 10.5281/zenodo.4284807., URL <https://github.com/ctkelley/SIAMFANLEquations.jl>, julia Package.
- [4] C. T. KELLEY, “Notebook for Solving Nonlinear Equations with Iterative Methods: Solvers and Examples in Julia,” <https://github.com/ctkelley/NotebookSIAMFANL> (2020); 10.5281/zenodo.4284687., URL <https://github.com/ctkelley/NotebookSIAMFANL>, iJulia Notebook.
- [5] C. T. KELLEY, “Solving Nonlinear Equations with Iterative Methods: Solvers and Examples in Julia,” (2020) Unpublished book ms, under contract with SIAM.
- [6] C. T. KELLEY, *Iterative Methods for Linear and Nonlinear Equations*, no. 16 in Frontiers in Applied Mathematics, SIAM, Philadelphia (1995).
- [7] Y. SAAD and M. SCHULTZ, “GMRES a generalized minimal residual algorithm for solving nonsymmetric linear systems,” *SIAM J. Sci. Stat. Comp.*, **7**, 856 (1986).
- [8] H. A. VAN DER VORST, “Bi-CGSTAB: A fast and smoothly converging variant to Bi-CG for the solution of nonsymmetric systems,” *SIAM J. Sci. Statist. Comput.*, **13**, 631 (1992).